View metadata, citation and similar papers at core.ac.uk

brought to you by CORE

東北大学機関リポジトリ
TOUR
Tohoku University Repository

Multistage recursive interleaver for turbo codes in DS-CDMA mobile radio

著者	安達　文幸
journal or publication title	IEEE Transactions on Vehicular Technology
volume	51
number	1
page range	88-100
year	2002
URL	http://hdl.handle.net/10097/46498

doi: 10.1109/25.992070

Multistage Recursive Interleaver for Turbo Codes in DS-CDMA Mobile Radio

Akira Shibutani, Hirohito Suda, *Member, IEEE*, and Fumiyuki Adachi, *Senior Member, IEEE*

***Abstract*—A multistage recursive block interleaver (MIL) is proposed for the turbo code internal interleaver. Unlike conventional block interleavers, the MIL repeats permutations of rows and columns in a recursive manner until reaching the final interleaving length. The bit error rate (BER) and frame error rate (FER) performance with turbo coding and MIL under frequency-selective Rayleigh fading are evaluated by computer simulation for direct-sequence code-division multiple-access mobile radio. The performance of rate-1/3 turbo codes with MIL is compared with pseudorandom and S-random interleavers assuming a spreading chip rate of 4.096 Mcps and an information bit rate of 32 kbps. When the interleaving length is 3068 bits, turbo coding with MIL outperforms the pseudorandom interleaver by 0.4 dB at an average BER of 10^{-6} on a fading channel using the ITU-R defined Vehicular-B power-delay profile with the maximum Doppler frequency of $f_D = 80$ Hz. The results also show that turbo coding with MIL provides superior performance to convolutional and Reed–Solomon concatenated coding; the gain over concatenated coding is as much as 0.6 dB.**

***Index Terms*—DS-CDMA, interleaver, turbo codes, W-CDMA.**

I. Introduction

WIDE-BAND direct-sequence code-division multiple access (W-CDMA) [1], [2] is attracting much attention for the third-generation mobile communications system called IMT-2000 [3]. Since all users use the same carrier frequency in CDMA systems, the radio links are not only power-limited but also interference-limited. Therefore, the link capacity is inversely proportional to the required signal energy per information bit to (background) noise plus interference power spectrum density ratio (E_b/N_0) [4]. This suggests that the use of powerful channel coding can contribute directly to increasing the link capacity. Initially, convolutional coding (CC) or convolutional and Reed–Solomon concatenated coding (CC+RS) were candidates for W-CDMA. However, the use of binary parallel concatenated coding or turbo coding [5], [6] has recently attracted much attention [7] due to its larger coding gain.

A turbo encoder consists of two or more recursive systematic convolutional (RSC) encoders separated by interleavers (internal interleaver). Turbo coding performance strongly depends on the length and structure of the internal interleaver. The internal interleaver assumed in [5] is a pseudorandom interleaver and offers relatively good performance. However, in some cases, the pseudorandom interleaver may generate poor permutation patterns (or interleaving patterns) that degrade the bit error rate (BER) and frame error rate (FER) performance. In this paper, we call these poor permutation patterns critical patterns (see Section II-D). To avoid these critical patterns, several interleaving methods have been proposed [8]–[10]. They are classified into two types: 1) searching for all or as many as possible pseudorandom interleaving patterns under a certain condition and 2) deterministic generation of interleaving patterns using schemes based on modified block interleaving. An example of 1) is the modified pseudorandom interleaver called the S-random interleaver [8], and examples of 2) are block interleavers with row sequence permutations as proposed in [9] and [10].

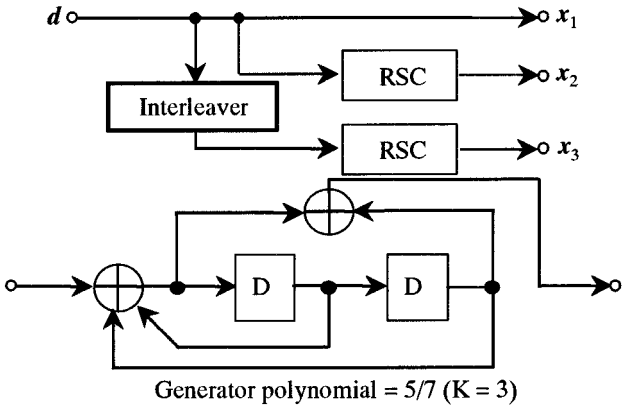

Fig. 1. Turbo encoder structure.

The design criteria of the internal interleaver for turbo-coded W-CDMA is to avoid the critical patterns for a wide range of interleaving lengths. For multimedia communications, code lengths with a wide generated range (for example, 300–8000 bits) are required. The S-random interleaver can be adopted for various interleaving lengths of turbo coding. However, there is increased computational complexity when searching for a good interleaving pattern in the case of a longer interleaver length. Compared to the S-random interleaver, interleaving pattern generation is much simpler for the deterministic block interleavers because they usually use very simple equations (for example, add or multiplication operations). However, algorithms that generate interleaving patterns that avoid the critical patterns for a wide range of interleaving lengths have not yet been thoroughly studied.

This paper proposes a multistage recursive block interleaver (MIL) that repeats permutations of rows and columns in a recursive manner until reaching the final interleaving length. MIL can generate good interleaving patterns avoiding the critical patterns for a wide range of interleaving lengths. We apply this MIL to turbo coding and evaluate by computer

Manuscript received August 3, 1999; revised August 13, 2001. This paper was presented in part at IEEE APCC/ICCS'98, Singapore, November 1998.

The authors are with the Wireless Laboratories, NTT Mobile Communications Network, Inc., 239-8536 Kanagawa-ken, Japan (e-mail: shibu@mlab.yrp.nttdocomo.co.jp).

Publisher Item Identifier S 0018-9545(02)00433-4.

0018-9545/02$17.00 © 2002 IEEE

Authorized licensed use limited to: TOHOKU UNIVERSITY. Downloaded on March 07,2010 at 19:35:57 EST from IEEE Xplore. Restrictions apply.

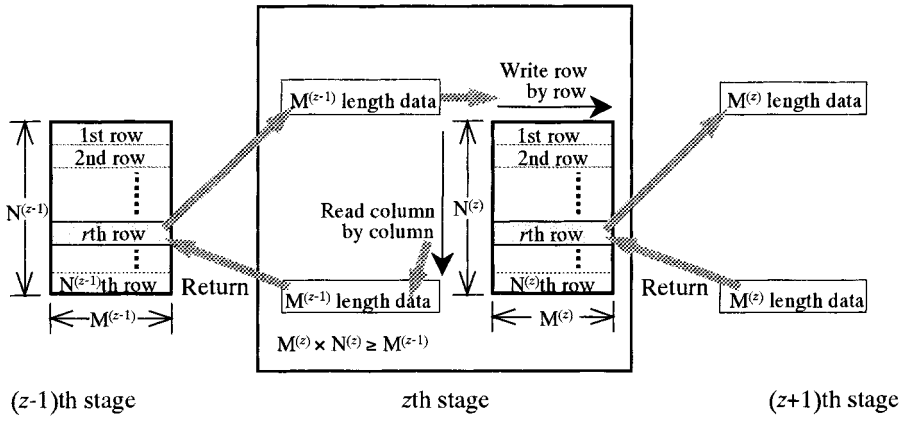

Fig. 2. Recursive process of MIL (only row permutation is shown). (The superscript$^{(x)}$ of $M^{(x)}$ denotes the stage number of the block interleaver, i.e., (x)th stage block interleaver has an interleaving pattern of $N^{(x)} \times M^{(x)}$.)

simulation the BER and FER performance of W-CDMA under frequency-selective Rayleigh-fading environments. Section II presents the principle and implementation of MIL. Section III describes the computer simulation model, and Section IV presents the simulation results. In Section IV, the BER and FER performances with turbo coding using MIL are compared to those using the S-random interleaver. Furthermore, the impact of various turbo-coding parameters (i.e., number of decoding iterations and interleaving length) and radio channel parameters (i.e., maximum Doppler frequency and power-delay profile shape) on the achievable BER and FER performance is discussed. We also compare the coding gains of turbo codes to those of CC+RS concatenated coding.

II. Multistage Recursive Interleaver

A. Principle

The turbo encoder with rate 1/3 and constraint length $K = 3$ considered in this paper is illustrated in Fig. 1 [1]. The RSC encoders have generator polynomials of 5/7 in octal notation. The data sequence $\boldsymbol{d} = (d_1, d_2, \ldots, d_{L_{\text{turbo}}})$ of length L_{turbo} bits is input into the encoder. The output of the turbo encoder is a systematic sequence $\boldsymbol{x}_1$ $(=\boldsymbol{d})$ and two parity sequences $\boldsymbol{x}_2$ and $\boldsymbol{x}_3$, where $\boldsymbol{x}_2$ and $\boldsymbol{x}_3$ are the outputs of RSC encoders without and with the internal interleaver, respectively. The desired characteristics for the internal interleaver are [6]:

1) avoiding critical patterns (see Section II-B);
2) having a high degree of randomness.

To produce good random interleaving patterns with a high degree of randomness while avoiding critical interleaving patterns, the MIL is designed as follows.

- Product permutation of each row and each column of data is performed at each stage.
- The permutation is repeated in a recursive manner until reaching the final interleaving length.

The recursive process is described below. Consider the row data permutation at the zth stage while referring to Fig. 2.

1) The row data sequence of length $M^{(z-1)}$ bits (stored in the previous, $(z-1)$th stage $N^{(z-1)} \times M^{(z-1)}$-block interleaver) is written to the zth stage $N^{(z)} \times M^{(z)}$-block interleaver row by row. In this paper, the superscript $^{(x)}$ of $M^{(x)}$ denotes the stage number of the block interleaver, i.e., the (x)th stage block interleaver has dimensions $N^{(x)} \times M^{(x)}$, where $N^{(x)}$ is the number of rows and $M^{(x)}$ is the number of columns.
2) The rth ($r = 1$ to $N^{(z)}$) row data sequence of the zth stage interleaver is read and passed on to the next stage $N^{(z+1)} \times M^{(z+1)}$ block interleaver row by row.
3) The $(z+1)$ stage block interleaver is read column by column and the data are returned to the rth row of the zth interleaver.

This recursive process is repeated until the final stage interleaving size is reached. A similar recursive process is applied to the column data permutation. In this paper, we call the $N^{(1)} \times M^{(1)}$-block interleaver the primary (first) interleaver. We call the $N^{(z)} \times M^{(z)}$ block interleaver with $z > 1$ a higher (the second, third, fourth, etc.) stage interleaver. The final stage interleaver has one of 2×2-, 2×3-, 3×2-, and 3×3-block interleaving patterns.

To describe the recursive interleaving process, the following operands are introduced in this paper.

1) $L[N \times M]$: An input sequence of length L bits is interleaved by an $N \times M$ block interleaver, where $L \leq N \times M$. This is the conventional block interleaver.

2) $L[N^{(z)}[N^{(z+1)} \times M^{(z+1)}] \times M^{(z)}]$: Write the L bit sequence to the $N^{(z)} \times M^{(z)}$ block interleaver row-by-row and then interleave each column sequence ($N^{(z)}$ bit length) using the same $N^{(z+1)} \times M^{(z+1)}$ block interleaver.

3) $L[N^{(z)} \times M^{(z)}[N^{(z+1)} \times M^{(z+1)}]]$: Write the L-bit sequence to the $N^{(z)} \times M^{(z)}$-block interleaver row-by-row and then interleave each row sequence ($M^{(z)}$ bit length) using the same $N^{(z+1)} \times M^{(z+1)}$ block interleaver. An example of the combination of $L[N^{(z)}[N^{(z+1)} \times M^{(z+1)}] \times M^{(z)}]$ and $L[N^{(z)} \times M^{(z)}[N^{(z+1)} \times M^{(z+1)}]]$ is shown in Fig. 3(a).

4) $L[N^{(z)} \times M^{(z)}[N_1^{(z+1)} \times M_1^{(z+1)}, N_2^{(z+1)} \times M_2^{(z+1)}, \ldots, N_{N^{(z)}}^{(z+1)} \times M_{N^{(z)}}^{(z+1)}]]$: Permute the bit order of the kth ($k = 1, 2, \ldots, N^{(z)}$) row data of the $M^{(z)}$-bit sequence by using the $N_k^{(z+1)} \times M_k^{(z+1)}$ block interleaver. An example is shown in Fig. 3(b).

5) $L[N^{(z)}[N_1^{(z+1)} \times M_1^{(z+1)}, N_2^{(z+1)} \times M_2^{(z+1)}, \ldots, N_{N^{(z)}}^{(z+1)} \times M_{N^{(z)}}^{(z+1)}] \times M^{(z)}]$: Permute the bit order of the kth ($k = 1, 2, \ldots, M^{(z)}$) column data of the

Authorized licensed use limited to: TOHOKU UNIVERSITY. Downloaded on March 07,2010 at 19:35:57 EST from IEEE Xplore. Restrictions apply.

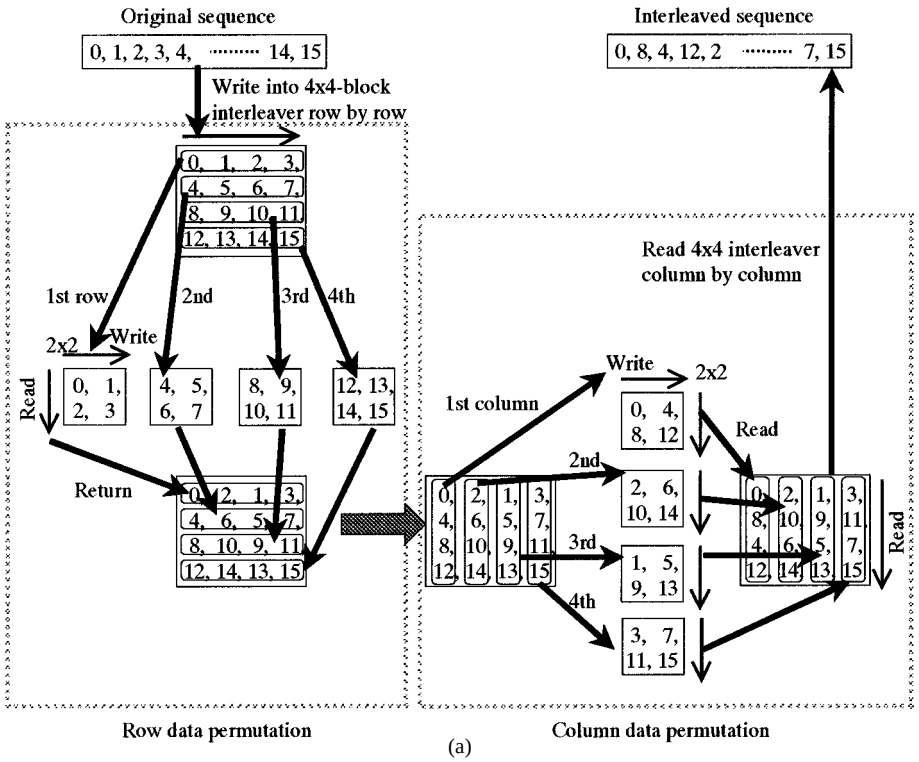

(a)

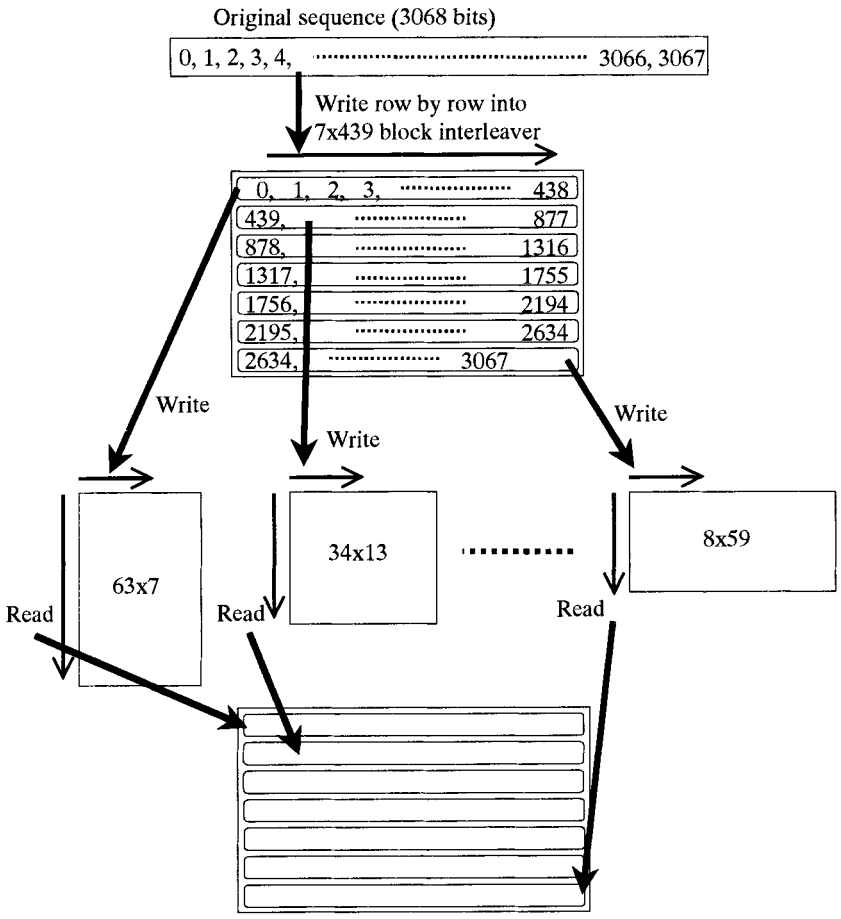

(b)

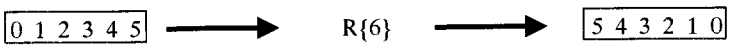

(c)

Fig. 3. Examples of interleaving operations.

Authorized licensed use limited to: TOHOKU UNIVERSITY. Downloaded on March 07,2010 at 19:35:57 EST from IEEE Xplore. Restrictions apply.

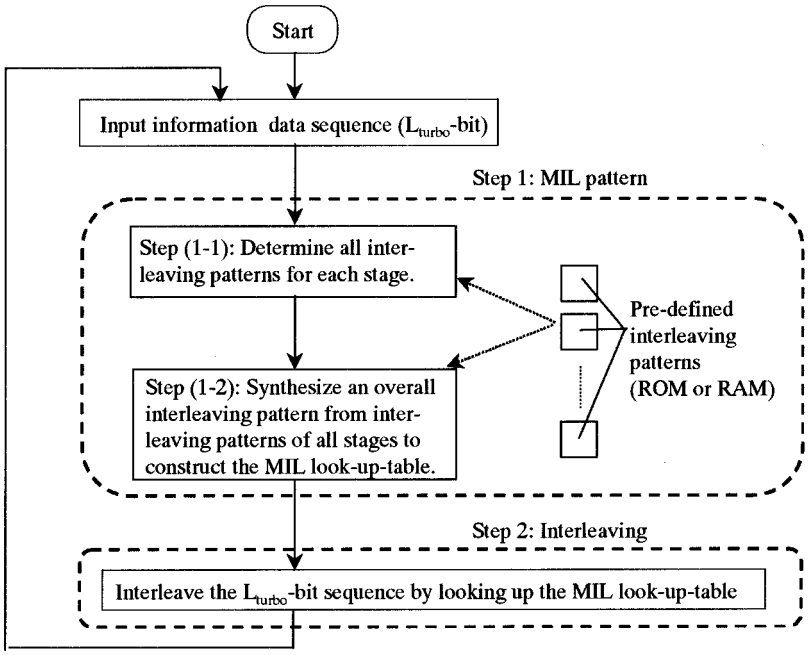

Fig. 4. MIL interleaving flowchart.

$N^{(z)}$-bit sequence by using the $N_k^{(z+1)} \times M_k^{(z+1)}$ block interleaver.

In addition, the following operand is introduced in this paper to randomize the interleaving pattern.

6) $R\{L\}$*:* Reverse the bit order of a sequence of L-bits. An example is shown in Fig. 3(c).

B. MIL Implementation

When turbo coding is applied to variable-bit-rate transmission as required in multimedia communications services, the interleaving length ($L_{\rm turbo}$ in bits) may be changed in each frame (defined in milliseconds). Therefore, a different MIL interleaving pattern must be generated for each frame. Attempting to store, in a read-only memory (ROM), the interleaving patterns for all possible interleaving lengths is not feasible. It is practical, however, to synthesize an interleaving pattern (when the frame data is input) and store it in a lookup table implemented by a random access memory (RAM) before interleaving each frame data.

The MIL has a complex construction because it has interleaved rows and columns multiplied in a recursive manner. The following describes a method for generating the MIL interleaving pattern in an efficient way. MIL interleaving is performed according to the flowchart shown in Fig. 4. The MIL interleaving flowchart comprises two steps:

Step 1) construct the MIL pattern;
Step 2) interleave based on the MIL lookup table, where a one-to-one mapping of the input bit to the output is stored.

Step 1) is performed once when the frame data sequence is input. We assume $L_{\rm turbo} > 300$. This is because that the performance of turbo codes with $L_{\rm turbo} > 300$ is better than that of the convolutional codes (constraint length of nine) [7]. Step 1) is further broken down into two substeps: Step (1-1) determines the interleaving patterns of the primary interleaver and higher stage interleavers (see Fig. 5) and Step (1-2) synthesizes the overall interleaving pattern using higher stage interleaving patterns (see Fig. 6). In Fig. 5, $\lfloor x \rfloor$ are the smallest integer larger than or equal to x and $\lceil x \rceil$ are the largest integer smaller than or equal to x, respectively. The resultant interleaver is represented by the equation shown at the bottom of the page, where PIP stands for the predefined interleaving pattern (each PIP is constructed in a recursive manner from the final stage interleavers and occupies less than 61 bits). In this example, $N^{(1)}[\text{PIP}] = R\{7[3 \times 3[2 \times 2]]\}$ and $M_{1-7}^{(2)}[\text{PIP}]$ represents the PIP with a length of $M_{1-7}^{(2)}$ bits, which is listed in Table I.

In Step (1-2), an overall interleaving pattern is synthesized from PIPs. How to synthesize the overall interleaving pattern is illustrated in Fig. 6. Let us consider the $N_k^{(z-1)}$ bit interleaving

$$L\Big[N^{(1)}[\text{PIP}] \times M^{(1)}\Big[N_1^{(2)}\Big[N_1^{(3)}[\cdots] \times M_1^{(3)}[\text{PIP}]\Big] \times M_1^{(2)}[\text{PIP}]\ ,$$
$$N_2^{(2)}\Big[N_2^{(3)}[\cdots] \times M_2^{(3)}[\text{PIP}]\Big] \times M_2^{(2)}[\text{PIP}],$$
$$\vdots$$
$$N_7^{(2)}\Big[N_7^{(3)}[\cdots] \times M_7^{(3)}[\text{PIP}]\Big] \times M_7^{(2)}[\text{PIP}]\Big]\Big]$$

Authorized licensed use limited to: TOHOKU UNIVERSITY. Downloaded on March 07,2010 at 19:35:57 EST from IEEE Xplore. Restrictions apply.

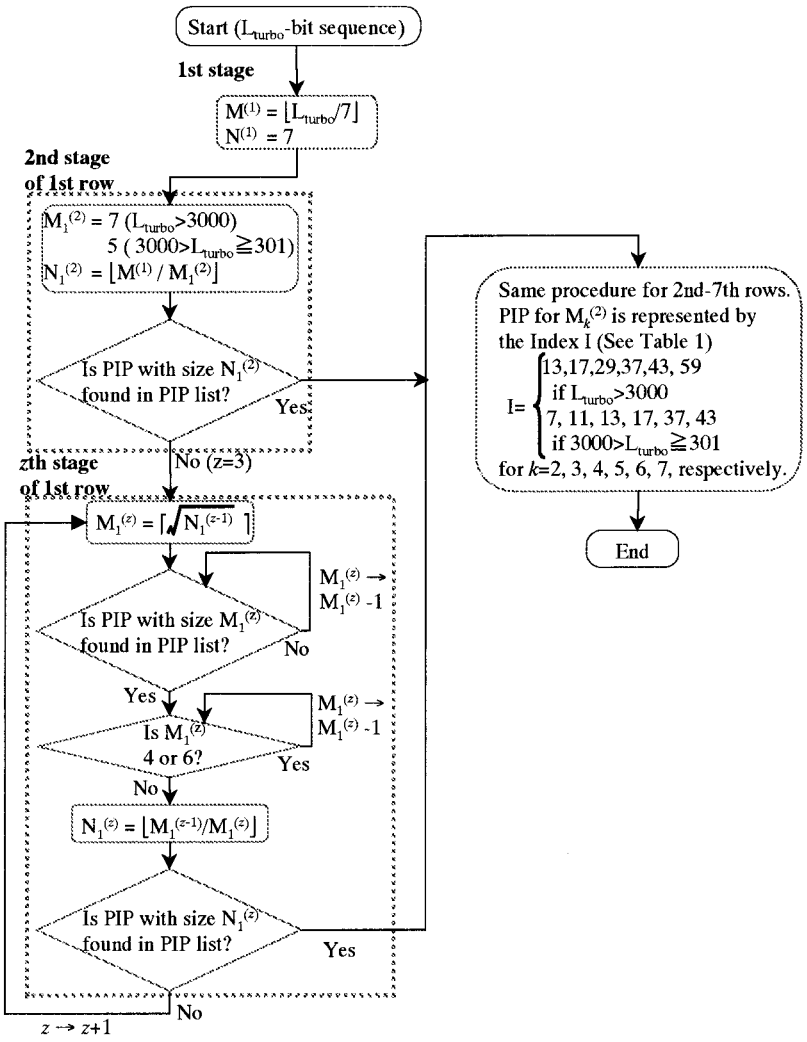

Fig. 5. Flowchart for finding PIPs used in each stage. $N^{(1)} = 7$ and the column data interleaving pattern is $R\{7[3 \times 3[2 \times 2]]\} = (4, 1, 5, 2, 6, 3, 0)$ for the input of (0, 1, 2, 3, 4, 5, 6).

pattern $A_k^{(z-1)}$ at the $(z-1)$th stage. It is synthesized from the $N_k^{(z)}$ bit pattern $A_k^{(z)}$, which was synthesized at the zth stage, and $M_k^{(z)}$ bit PIP $B_k^{(z)}$

$$A_k^{(z-1)}[i] = M_k^{(z)} \times A_k^{(z)} \left[i \bmod N_k^{(z)} \right] + B_k^{(z)} \left[i/N_k^{(z)} \right], \quad 0 \le i < N_k^{(z-1)}. \quad (1)$$

If $N_k^{(z-1)} < N_k^{(z)} \times M_k^{(z)}$, we prune some of the elements of $A_k^{(z-1)}[i]$, i.e., the value of the elements larger than or equal to $N_k^{(z-1)}$. The above step is repeated until the $M^{(1)}$ bit interleaving pattern of the kth row of the primary (first stage) interleaver is synthesized. The same procedure is performed for $k = 1$–7. Finally, the overall interleaving pattern C is generated by $N^{(1)}$-bit PIP B and the synthesized $M^{(1)}$-bit interleaving patterns $A_k^{(1)}$, $k = 1$–7

$$C[i] = M^{(1)} \times B \left[i \bmod N^{(1)} \right] + A^{(1)}_{B[i \bmod N^{(1)}]+1} \left[i/N^{(1)} \right], \quad 0 \le i < L_{\text{turbo}}. \quad (2)$$

If $L_{\text{turbo}} < N^{(1)} \times M^{(1)}$, we again prune some of the elements of C, i.e., the value of the elements larger than or equal to L_{turbo}. In Step 2), the L_{turbo} bit sequence is interleaved simply by accessing the MIL lookup table.

C. Synthesizing 3068-Bit MIL Pattern as an Example

The synthesis of a 3068-bit MIL pattern is illustrated in Fig. 7. The value of $N^{(1)}$ is set to seven. Since $M^{(1)} = \lfloor L_{\text{turbo}}/7 \rfloor = 439$, the primary (first stage) interleaver is a 7×439 ($=N^{(1)} \times M^{(1)}$) block interleaver. The PIPs necessary to synthesize the interleaving patterns of each stage are found from Table I. To increase the degree of randomness, the seven interleavers of the second stage, each corresponding to one of the seven rows of the first stage, are all different. First, we design the second-stage block interleaver corresponding to the first row of the first stage. The value of $M_1^{(2)}$ is seven (since $L_{\text{turbo}} > 3000$ bits) and $N_1^{(2)} = \lfloor M^{(1)}/M_1^{(2)} \rfloor = \lfloor 439/7 \rfloor = 63$. The PIP of length 63 ($=N_1^{(2)}$) is not found in the PIP table of Table I. Therefore, we go to the third stage. $M_1^{(3)}$ is the largest integer smaller than or equal to the square root of $N_1^{(2)}$ and $M_1^{(3)} = 7$. Thus, $N_1^{(3)} = \lfloor N_1^{(2)}/M_1^{(3)} \rfloor = \lfloor 63/7 \rfloor = 9$. The PIP of length nine is found from Table I, and we do not need to go to a higher stage. The same procedure is repeated for the second row, third row , . . . , seventh row of the first-stage block interleaver.

After finding all PIPs of all stages, the overall interleaving pattern is synthesized in a recursive manner starting from the

Authorized licensed use limited to: TOHOKU UNIVERSITY. Downloaded on March 07,2010 at 19:35:57 EST from IEEE Xplore. Restrictions apply.

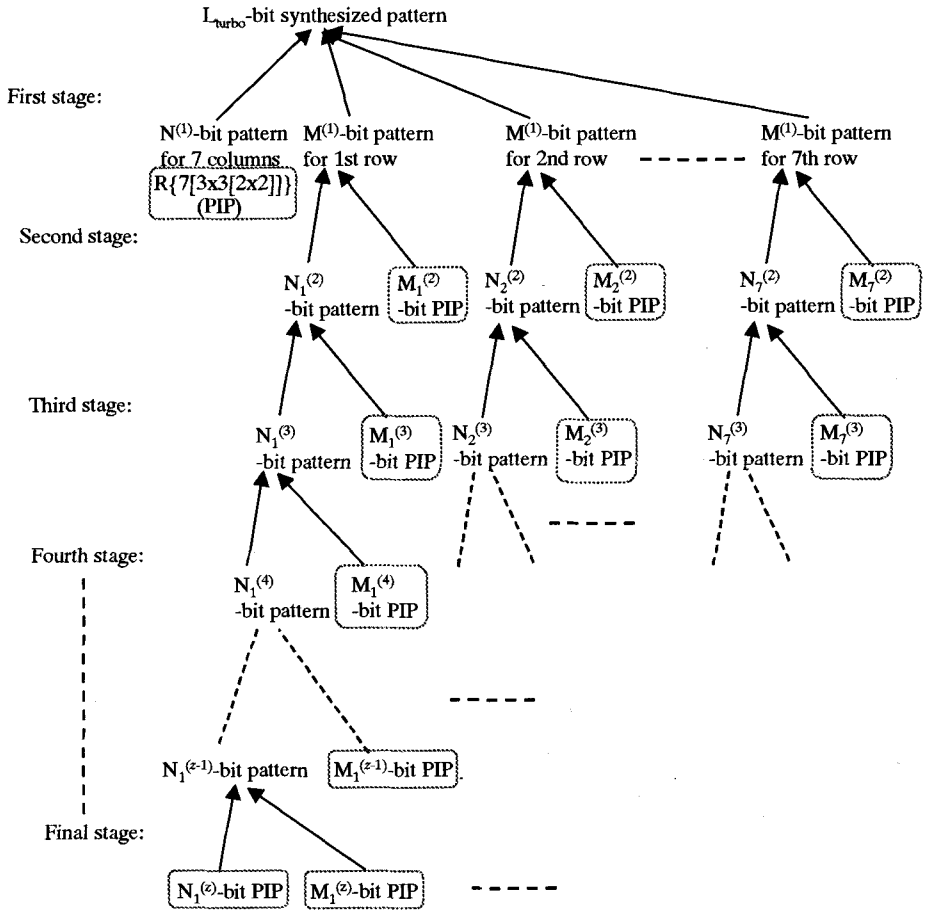

Fig. 6. Synthesis of overall interleaving pattern.

third stage [see Fig. 7(b)]. The second-stage interleaving pattern $A_1^{(2)}$ of length $N_1^{(2)} = 63$ is synthesized using the PIPs of length $N_1^{(3)} = 9$ and of length $M_1^{(3)} = 7$ using (1) [note that $A_1^{(3)}$ is PIP in (1)]. Thus, (1) can be rewritten as

$$A_1^{(2)}[i] = 7 \times A_1^{(3)}[i \bmod 9] + B_1^{(3)}[i/9], \quad 0 \le i < 63$$

where $A_1^{(3)}$ and $B_1^{(3)}$ are given by the patterns defined in index $I = 9$ and index $I = 7$ of Table I, respectively. The first-stage interleaving pattern $A_1^{(1)}$ of length $M^{(1)} = 439$ is synthesized using the synthesized interleaving patterns $A_1^{(2)}$ of length $N_1^{(2)} = 63$ and PIP of length $M_1^{(2)} = 7$ using (1) (pruning is necessary to adjust the sequence length to 439). Finally, by using the PIP of length $N^{(1)} = 7$ for column permutation and the synthesized seven row-permutation patterns $A_1^{(1)}, \ldots, A_7^{(1)}$ of length $M^{(1)} = 439$, the overall interleaving pattern can be synthesized using (2). The synthesized MIL pattern is represented as shown in (3) at the bottom of the page.

D. Avoiding Critical Patterns

1) Description of Critical Patterns:

a) Weight-2 information data: The most critical interleaving pattern for the turbo encoder in Fig. 1 is found to be the one that interleaves the input sequence in such a way that pairs of bits with a distance of 3 bits are separated by a distance of 3 bits in the case of a weight-2 information data sequence [8], [9]. This is demonstrated below. Consider that a 16-bit-information data sequence having a weight of two

$$\boldsymbol{d} = \{1,0,0,1,0,0,0,0,0,0,0,0,0,0,0,0\}$$

$$
\begin{aligned}
&3068[R\{7[3\times3[2\times2]]\} && \text{(for the columns of the primary interleaver)}\\
&\quad\times439[63[9[R\{2\}\times5[2\times3]]\times7[3\times3[2\times2]]]\times7[3\times3[2\times2]] && \text{(for the 1st row of the primary interleaver)}\\
&\qquad 34[7[3\times3[2\times2]]\times5[2\times3]]\times13[2\times7[3\times3[2\times2],\\
&\qquad 3[3\times1, 2\times R\{2\}, 2\times R\{2\}]\times3[R\{3\}\times1, R\{3\}\times1, 3\times1]]], && \text{(2nd row)}\\
&26[6[3\times2]\times5[2\times3]]\times17[4[2\times2, 4\times1, 4\times1, 4\times1, 4\times1]\times5[3\times2]], && \text{(3rd row)}\\
&16[6[3\times2]\times R\{3[2\times2]\}]\times29[5[3\times2]\times7[3\times3[2\times2]]], && \text{(4th row)}\\
&12[4[2\times R\{2\}]\times R\{3[2\times2]\}]\times37[7[3\times3]\times6[3\times2]], && \text{(5th row)}\\
&11[3\times5[3\times2]]\times43[4[2\times2]\times11[3\times5[3\times2]]], && \text{(6th row)}\\
&8[4[2\times2]\times2]\times59[9[R\{2\}\times5[2\times3]]\times7[3\times3]] && \text{(7th row)]]}. \qquad (3)
\end{aligned}
$$

Authorized licensed use limited to: TOHOKU UNIVERSITY. Downloaded on March 07,2010 at 19:35:57 EST from IEEE Xplore. Restrictions apply.

TABLE I
PIP LIST

Index	Operand	Interleaving pattern for the input of (0, 1, 2, 3, ...)
I=2	R{2}	1, 0
3	R{3[2x2]}	1, 2, 0
4	4[2xR{2}]	1, 3, 0, 2
5	5[2x3]	0, 3, 1, 4, 2
6	6[3x2]	0, 2, 4, 1, 3, 5
7	7[3x3[2x2]]	0, 3, 6, 2, 5, 1, 4
8	8[4[2x2]x2]	0, 4, 2, 6, 1, 5, 3, 7
9	9[R{2}x5[2x3]]	5, 0, 8, 3, 6, 1, 4, 7, 2
11	11[3x5[3x2]]	0, 5, 10, 2, 7, 4, 9, 1, 6, 3, 8
13	13[2x7[3x3[2x2], 3[3x1,2xR{2},2xR{2}]x 3[R{3}x1,R{3}x1,3x1]]]	0, 9, 3, 12, 6, 2, 11, 5, 8, 1, 10, 4, 7
17	17[4[2x2,4x1,4x1,4x1,4x1] x5[3x2]]	0, 10, 5, 15, 2, 7, 12, 4, 9, 14, 1, 6, 11, 16, 3, 8, 13
20	20[4[2xR{2}]x5[2x3]]	5, 15, 0, 10, 8, 18, 3, 13, 6, 16, 1, 11, 9, 19, 4, 14, 7, 17, 2, 12
29	29[5[3x2]x7[3x3[2x2]]]	0, 14, 28, 7, 21, 3, 17, 10, 24, 6, 20, 13, 27, 2, 16, 9, 23, 5, 19, 12, 26, 1, 15, 8, 22, 4, 18, 11, 25
37	37[7[3x3]x6[3x2]]	0, 18, 36, 6, 24, 12, 30, 2, 20, 8, 26, 14, 32, 4, 22, 10, 28, 16, 34, 1, 19, 7, 25, 13, 31, 3, 21, 9, 27, 15, 33, 5, 23, 11, 29, 17, 35
43	43[4[2x2]x11[3x5[3x2]]]	0, 22, 11, 33, 5, 27, 16, 38, 10, 32, 21, 2, 24, 13, 35, 7, 29, 18, 40, 4, 26, 15, 37, 9, 31, 20, 42, 1, 23, 12, 34, 6, 28, 17, 39, 3, 25, 14, 36, 8, 30, 19, 41
47	47[7[3x3]x7[3x3]]	0, 21, 42, 7, 28, 14, 35, 3, 24, 45, 10, 31, 17, 38, 6, 27, 13, 34, 20, 41, 1, 22, 43, 8, 29, 15, 36, 4, 25, 46, 11, 32, 18, 39, 2, 23, 44, 9, 30, 16, 37, 5, 26, 12, 33, 19, 40
53	53[5[2x3]x11[3x5[3x2]]]	0, 33, 11, 44, 22, 5, 38, 16, 49, 27, 10, 43, 21, 32, 2, 35, 13, 46, 24, 7, 40, 18, 51, 29, 4, 37, 15, 48, 26, 9, 42, 20, 31, 1, 34, 12, 45, 23, 6, 39, 17, 50, 28, 3, 36,14, 47, 25, 8, 41, 19, 52, 30
59	59[9[R{2}x5[2x3]]x7[3x3]]	35, 0, 56, 21, 42, 7, 28, 49, 14, 38, 3, 24, 45, 10, 31, 52, 17, 41, 6, 27, 48, 13, 34, 55, 20, 36, 1, 57, 22, 43, 8, 29, 50, 15, 39, 4, 25, 46, 11, 32, 53, 18, 37, 2, 58, 23, 44, 9, 30, 51, 16, 40, 5, 26, 47, 12, 33, 54, 19
61	61[5[2x3]x 13[5[2x3]x3[2x2]]]	0, 39, 13, 52, 26, 9, 48, 22, 35, 3, 42, 16, 55, 29, 12, 51, 25, 38, 6, 45, 19, 58, 32, 2, 41, 15, 54, 28, 11, 50, 24, 37, 5, 44, 18, 57, 31, 8, 47, 21, 60, 34, 1, 40, 14, 53, 27, 10, 49, 23, 36, 4, 43, 17, 56, 30, 7, 46, 20, 59, 33

is input to an RSC encoder. The output $\boldsymbol{x}_2$ of Fig. 1 is

$$\boldsymbol{x}_2 = \{1,1,1,1,0,0,0,0,0,0,0,0,0,0,0,0\}$$

which has the Hamming weight $\boldsymbol{H}$ of four. If the input sequence is interleaved to {1, 0, 0, 0, 0, 0, 0, 0, 0, 0, 0, 0, 0, 0, 0, 1}, the RSC decoder output $\boldsymbol{x}_3$ is

$$\boldsymbol{x}_3 = \{1,1,1,0,1,1,0,1,1,0,1,1,0,1,1,1\}.$$

In this case, the Hamming weight of the encoded sequence $(\boldsymbol{x}_1\boldsymbol{x}_2\boldsymbol{x}_3)$ is $\boldsymbol{H} = 2(\boldsymbol{d}) + 4(\boldsymbol{x}_2) + 12(\boldsymbol{x}_3) = 18$ [6]. In other words, even if one RSC produces a redundant sequence with a lower weight, the other can produce a redundant sequence with a larger weight, thereby producing an overall codeword with a large weight. However, if the input sequence is interleaved to { 0, 1, 0, 0, 1, 0, 0, 0, 0, 0, 0, 0, 0, 0, 0, 0} by the interleaver, the RSC encoder output $\boldsymbol{x}_3$ is

$$\boldsymbol{x}_3 = \{0,1,1,1,1,0,0,0,0,0,0,0,0,0,0,0\}.$$

In this case, $\boldsymbol{H} = 2(\boldsymbol{d}) + 4(\boldsymbol{x}_2) + 4(\boldsymbol{x}_3) = 10$. Our computer simulation shows that when $\boldsymbol{H} = 18$, the BER floor value decreases almost 200 times compared to that when $\boldsymbol{H} = 10$.

b) Weight-3 information data: In the case of a weight-3 information data sequence, the most critical interleaving pattern for the turbo encoder in Fig. 1 is found to be the one that interleaves the input sequence in such a way that consecutive 3 bits are interleaved to consecutive 3 bits. This is demonstrated below. Consider that a 16-bit-information data sequence having a weight of three

$$\boldsymbol{d} = \{1,1,1,0,0,0,0,0,0,0,0,0,0,0,0,0\}$$

is input to an RSC encoder. The output $\boldsymbol{x}_2$ of Fig. 1 is

$$\boldsymbol{x}_2 = \{1,0,1,0,0,0,0,0,0,0,0,0,0,0,0,0\}$$

which has the Hamming weight $\boldsymbol{H}$ of two. The same is true for $\boldsymbol{x}_3$ if the input sequence is interleaved to $\{1,1,1,0,0,0,0,0,$ $0,0,0,0,0,0,0,0\}$. In this case, the Hamming weight of the encoded sequence $(\boldsymbol{x}_1\boldsymbol{x}_2\boldsymbol{x}_3)$ is $\boldsymbol{H} = 3(\boldsymbol{d}) + 2(\boldsymbol{x}_2) + 2(\boldsymbol{x}_3) = 7$ [6].

We call the following patterns the critical patterns in this paper [8], [9].

1) The one that interleaves the input sequence in such a way that pairs of bits with a distance of 3 bits are separated by a distance of 3 bits (weight-2 information data).

Authorized licensed use limited to: TOHOKU UNIVERSITY. Downloaded on March 07,2010 at 19:35:57 EST from IEEE Xplore. Restrictions apply.

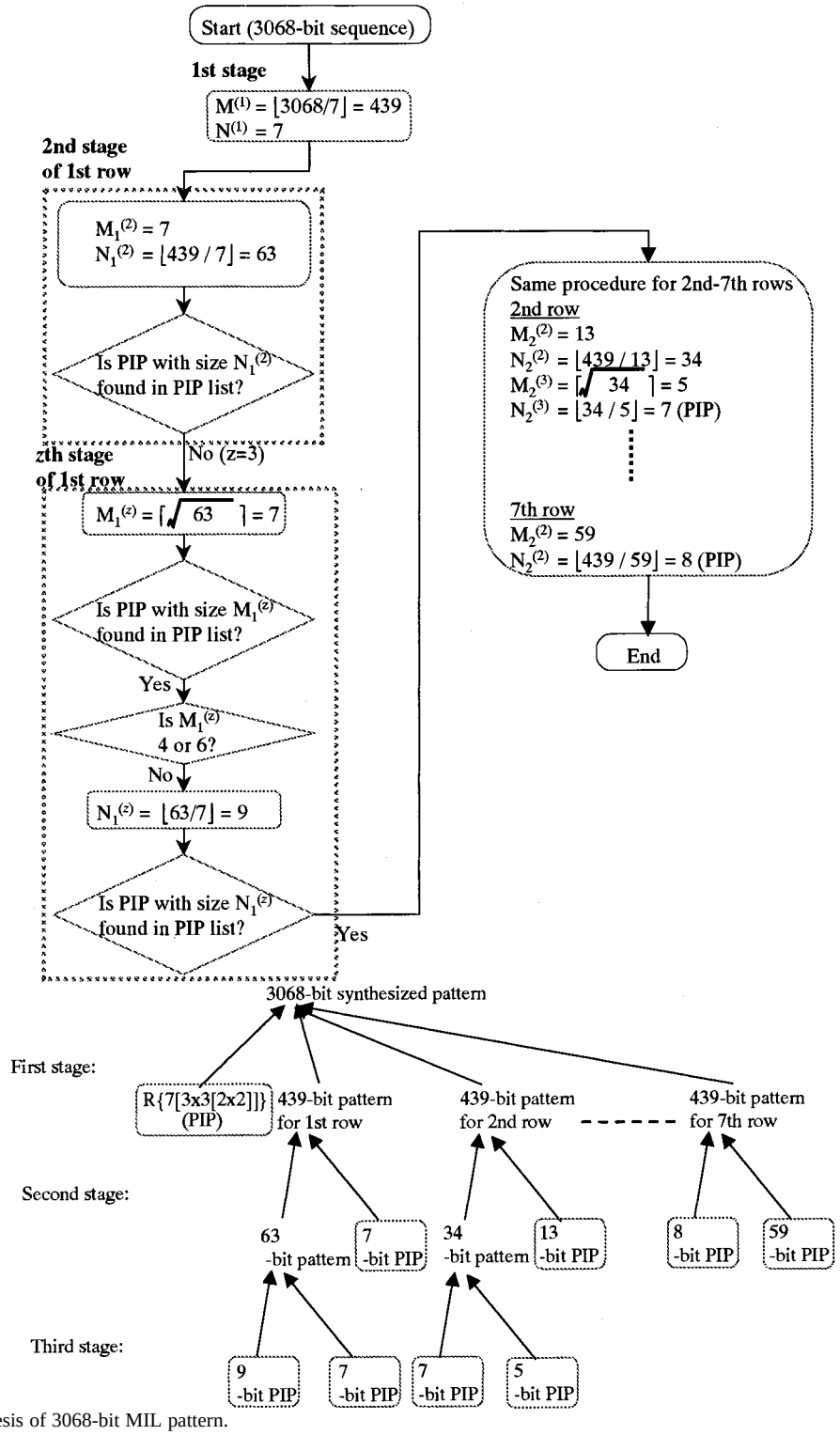

Fig. 7. Example of synthesis of 3068-bit MIL pattern.

2) The one that interleaves the input sequence in such a way that consecutive 3 bits are interleaved to consecutive 3 bits (weight-3 information data).

2) Description of Avoiding Critical Patterns: How the most critical pattern can be avoided is explained below assuming $L_{\text{turbo}} = 3068$ bits. Our MIL, designed for the turbo encoder shown in Fig. 1, has a primary (first stage) block interleaver with seven rows. In the first stage, the first to sixth rows have 439 bits each and the seventh row has 434 bits [see Fig. 3(b)]. After interleaving, the sequences are stored in all rows as described previously, and then the column data are interleaved. In our MIL, the column data interleaving pattern is $R\{7[3 \times 3[2 \times 2]]\} = (4,1,5,2,6,3,0)$ for all seven columns. Remember that the primary interleaver is read column by column to output the interleaved sequence. This means that when reading each column entry, the bit stored in the fifth row appears first, followed by, in order, bits stored in the second, sixth, third, seventh, fourth, and first rows. In

Authorized licensed use limited to: TOHOKU UNIVERSITY. Downloaded on March 07,2010 at 19:35:57 EST from IEEE Xplore. Restrictions apply.

TABLE II
SIMULATION PARAMETERS

Chip rate		4.096Mcps
Modulation	Spreading	QPSK, long pseudo-random sequence
	Data	QPSK
Channel interleaver		Turbo: MIL cc+RS: 72x128 block interleaver(32kbps, 80ms)
Channel coding		Turbo: R=1/3, K=3 8 iterations, Soft-in/Soft-out Viterbi decoder CC+RS: Convolutional coding (R=1/3, K=9) and (36, 32) Reed-Solomon coding on GF(2^8)
Information rate		32kbps
Transmit power control (TPC)		SIR-based closed loop fast TPC [12]
Diversity	Space	2-branch antenna diversity
	RAKE	4-finger coherent RAKE
Propagation model		Vehicular B profile [11]

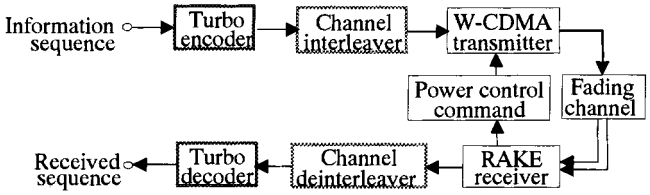

Fig. 8. W-CDMA reverse link model.

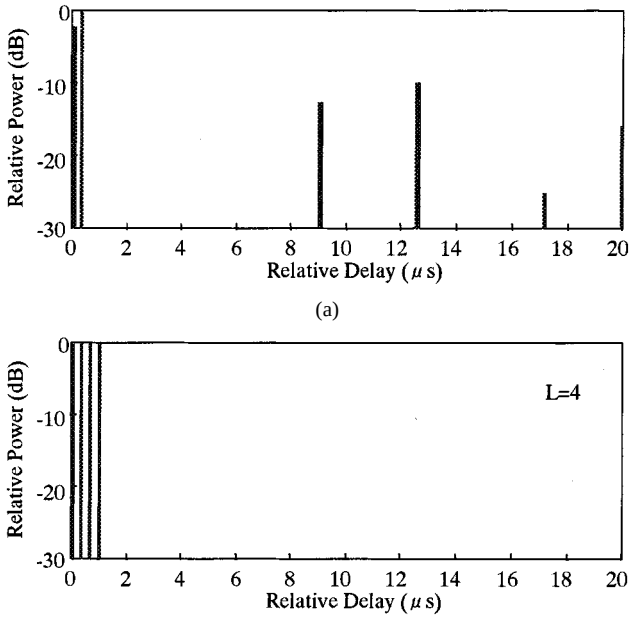

(a)

(b)

Fig. 9. Power-delay profiles. (a) Vehicular B ($L = 6$). (b) Uniform ($L = 4$ case).

the case of weight-2 information data, the pairs of bits with a distance of three in the interleaved sequence (the pairs of bits are, for example, two bits read from the fifth and third rows) correspond to the bits with a distance of more than 439 in the input sequence. Furthermore, in the case of weight-3 information data, consecutive 3 bits in the interleaved sequence (the consecutive 3 bits are, for example, three bits read from the fifth, second, and sixth rows) correspond to nonconsecutive 3 bits in the input sequence because at least 1 bit is separated from the others with a distance of more than 439. Thus, the two critical patterns can be avoided.

III. COMPUTER SIMULATION

The improvement in the average BER and FER performance with turbo coding by using the MIL is examined by computer simulation assuming a power-controlled W-CDMA reverse link under frequency-selective Rayleigh fading. The simulated BER and FER performance are compared with those achieved using a random interleaver. MIL can also realize channel interleaving, so the effects of using the MIL as a turbo internal interleaver and as a channel interleaver are also evaluated.

A. W-CDMA Reverse Link Model

Fig.8 shows the W-CDMA reverse link model [1] considered hereafter. Table II shows the simulation parameters. We assume a single mobile user that is continuously transmitting data at 32 kbps. The information data to be transmitted are divided into a sequence of data frames, each L_{turbo} bits long (T_{turbo} ms in time). The data sequence is first turbo coded frame by frame. Turbo coding with the rate $R = 1/3$ and constraint length $K = 3$ is assumed (see Fig. 1). Channel interleaving is then applied before data modulation using quaternary phase-shift keying (QPSK). The coded QPSK symbols are mapped over multiple slots of the radio channel; each slot has four pilot symbols at its beginning and is 0.625 ms long [1]. The resultant QPSK-modulated symbol sequence of 64 k symbol/s (sps) is spread by a 4.096-Mchip/s (cps) complex, long, pseudorandom spreading sequence (the spreading factor is 64) and then transmitted over a frequency-selective Rayleigh-fading channel. Signal-to-interference ratio based closed-loop fast transmit power control (TPC) [12] is applied; the power-control step size is 1 dB and the power-control rate is 1600 Hz.

Two fading channels with different power-delay profiles are considered: The ITU-specified Vehicular B power-delay profile (six discrete paths) [11] and an L-path uniform power-delay profile $L = 1$–8. These power-delay profiles are illustrated in Fig. 9. Two spatially separated antennas and a four-finger coherent RAKE combiner are used at the base-station receiver.

Authorized licensed use limited to: TOHOKU UNIVERSITY. Downloaded on March 07,2010 at 19:35:57 EST from IEEE Xplore. Restrictions apply.

TABLE III
COMBINATION OF TURBO AND CHANNEL INTERLEAVERS

	Turbo interleaver	Channel interleaver
RND-BLK	pseudo random	72x128 block interleaver
RND-MIL	pseudo random	MIL
MIL-BLK	MIL	72x128 block interleaver
MIL-MIL	MIL	MIL
SRI22-BLK	S-random interleaver	72x128 block interleaver

Channel estimation for the coherent RAKE combiner is performed by simply averaging the eight received pilot symbols of two consecutive slots [13]. The RAKE-combiner output sample is deinterleaved and turbo decoded. Two soft-in/soft-out Viterbi decoders are employed in the turbo decoder [7]. The decoded BER performance improves as the number of decoding iterations increases. However, since the BER improvement is basically saturated at eight iterations [7], turbo decoding with eight iterations is assumed in this simulation.

B. Interleaver Design

We consider four turbo internal interleaver and channel interleaver combinations, as shown in Table III. The MIL turbo interleaver of length $L_{\text{turbo}} = 3068$ bits (corresponding interleaving length T_{turbo} in time is 80 ms) is described by (3). On the other hand, the pseudorandom interleaver changes its interleaving pattern frame by frame.

The MIL channel interleaver of length $L_{\text{channel}} = 9216$ bits (corresponding length T_{channel} in time is 80 ms) is represented as 9216[72[9[3 × 3] × 8[4[2 × 2] × 2]] × 128[16[4[2 × 2] × 4[2 × 2]] × 8[4[2 × 2] × 2]]]. The number of columns in the primary stage equals the number of radio channel slots per data frame (i.e., 128). The higher stage interleavers are designed to be as square as possible because square interleavers provide better performance.

C. Simulation Results

The average BER, FER, and E_b/N_0 values per antenna were first measured for different target values of fast TPC; the resulting BER and FER performance curves are plotted as a function of the average E_b/N_0 per antenna in Fig. 10. It can be clearly seen from this figure that the combination of MIL-MIL provides the best performance, especially when BER $< 10^{-4}$. Moreover, an approximate 0.4-dB reduction in the required E_b/N_0 for the average BER $= 10^{-6}$ is achieved compared to RND-BLK (random interleaver for the turbo interleaver and block interleaver for the channel interleaver).

It is well known that the S-random interleaver with a large value of S achieves better BER performance than the pseudorandom interleaver [8]. The S-random interleaver is designed to separate (by more than S bits) all the neighboring bits within a distance of S bits from the target input bit. An S-random interleaving pattern is generated as follows. First, the output position of the target input bit is randomly selected. The selected position is compared to the selected (determined) output positions of S previous input bits, to check if the S-rule is satisfied. If the current selection does not satisfy the S rule, the current selection is rejected and a new selection is made. This process is repeated until output positions of all bits in the input sequence are determined.

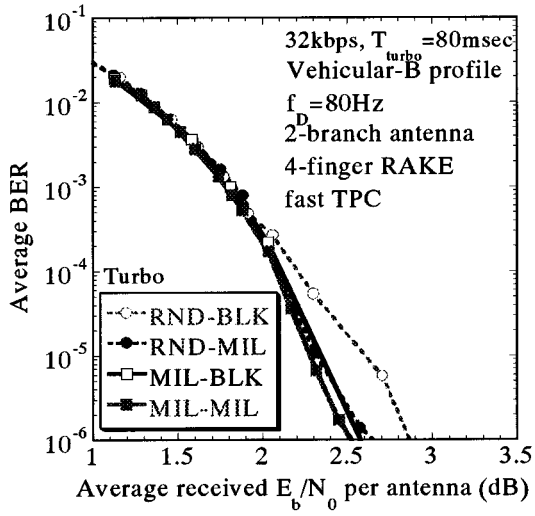

(a)

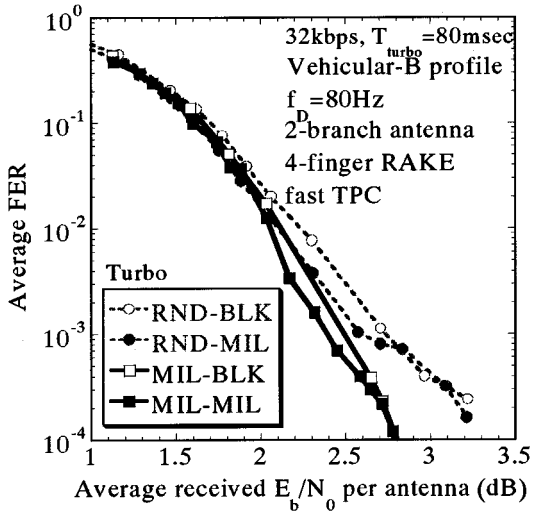

(b)

Fig. 10. Performance comparison between different combinations of turbo and channel interleaver. (a) BER and (b) FER.

With a large value of S, since the S-random interleaver can avoid the severe critical patterns by applying the S-rule, it can offer better BER performance than the pseudorandom interleaver can. However, larger computational complexity is incurred in searching for a good interleaving pattern in the case of a long interleaver length. This is because the number ofposition-reselection operations increases almost exponentially with the interleaving length. Fig. 11 compares the BER and FER performance achievable with MIL to that offered by the S-random interleaver (SRI). The S-random parameter is $S = 22$. It can be seen from this figure that the performances of MIL-BLK and MIL-MIL are better than that of SRI22-BLK (S-random interleaver for the turbo interleaver and block interleaver for the channel interleaver) despite the deterministic generation of MIL patterns. MIL-BLK and MIL-MIL reduce the E_b/N_0 required to achieve the BER $= 10^{-6}$ by more than 0.2 and 0.3 dB, respectively, from that with SRI22-BLK. We also have performed computer simulations on the BER and

Authorized licensed use limited to: TOHOKU UNIVERSITY. Downloaded on March 07,2010 at 19:35:57 EST from IEEE Xplore. Restrictions apply.

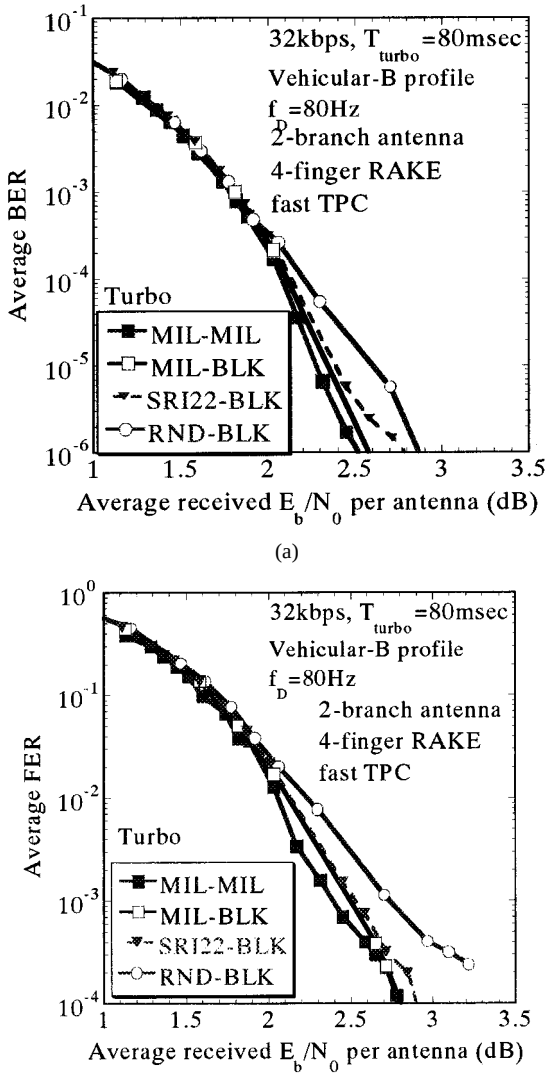

(a)

(b)

Fig. 11. Performance comparison with SRI ($S = 22$). (a) BER and (b) FER.

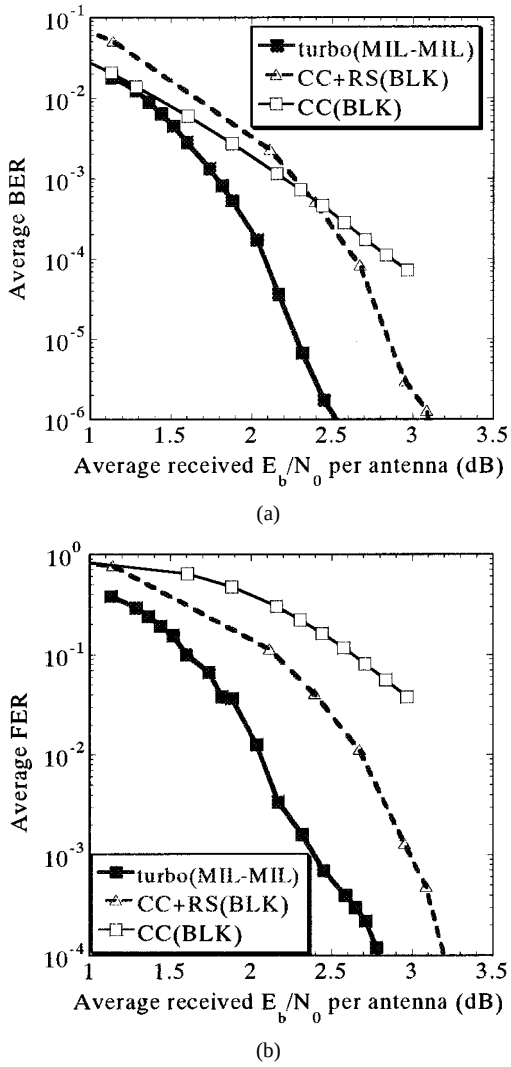

(a)

(b)

Fig. 12. Performance comparison with convolutional coding (CC) and concatenated convolutional and RS coding (CC+RS). (a) BER and (b) FER.

FER performances achievable with MIL, SRI22, and RND in the additive white Gaussian noise channels. It has been found that MIL provides the same performance as (or slightly better than) the S-random interleaver.

Fig. 12 compares the BER and FER performance levels of turbo coding with MIL-MIL to those of convolutional coding (CC) and CC+RS. The parameters of CC are $R =$ rate $1/3$ with a constraint length of $K = 9$, and (36, 32) RS coding with 8 bits/symbol is assumed. For CC and CC+RS, a block interleaver of 72×128 was used for the channel interleaving. Furthermore, a block interleaver of 144×8 symbols was used for the outer interleaver [1] for CC+RS. It can be seen from Fig. 12 that turbo coding with MIL-MIL reduces the required E_b/N_0 for BER $= 10^{-6}$ by more than 0.6 dB compared to CC+RS.

So far, we have assumed an interleaving length of $L_{\text{turbo}} = 3068$ bits ($T_{\text{turbo}} = 80$ ms). The impact that the value of L_{turbo} has on the required E_b/N_0 for the average BER $= 10^{-6}$ was evaluated. The results are plotted in Fig. 13 for four different L_{turbo} values: 380 bits ($T_{\text{turbo}} = 10$ ms), 760 bits (20 ms), 1520 bits (40 ms), and 3068 bits (80 ms). The interleaving patterns of the MIL channel interleaver used in this simulation are shown in the equation at the bottom of the page. The interleaving patterns of the conventional block channel interleaver are 72×16 (10 ms), 72×32 (20 ms), 72×64 (40 ms), and 72×128 (80 ms). Fig.13 also plots the results of CC+RS concatenated coding. It can be clearly seen that as the interleaving

$$
\begin{aligned}
&72[9[3\times 3]\times 8[4[2\times 2]\times 2]]\times 16[4[2\times 2]\times 4[2\times 2]] && (10\text{ ms})\\
&72[9[3\times 3]\times 8[4[2\times 2]\times 2]]\times 32[8[4[2\times 2]\times 2]\times 4[2\times 2]] && (20\text{ ms})\\
&72[9[3\times 3]\times 8[4[2\times 2]\times 2]]\times 64[8[4[2\times 2]\times 2]\times 8[4[2\times 2]\times 2]] && (40\text{ ms})\\
&72[9[3\times 3]\times 8[4[2\times 2]\times 2]]\times 128[16[4[2\times 2]\times 4[2\times 2]]\times 8[4[2\times 2]\times 2]]] && (80\text{ ms}).
\end{aligned}
$$

Authorized licensed use limited to: TOHOKU UNIVERSITY. Downloaded on March 07,2010 at 19:35:57 EST from IEEE Xplore. Restrictions apply.

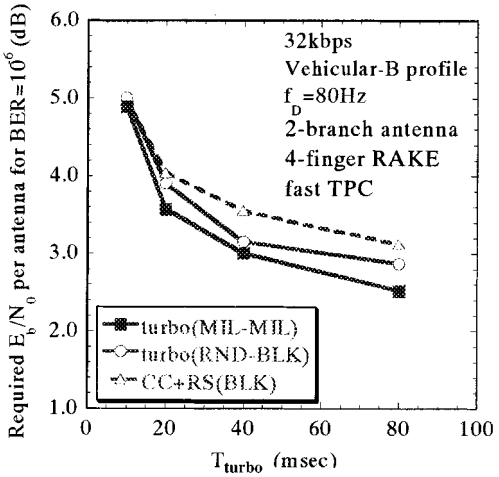

Fig. 13. Impact of interleaving size.

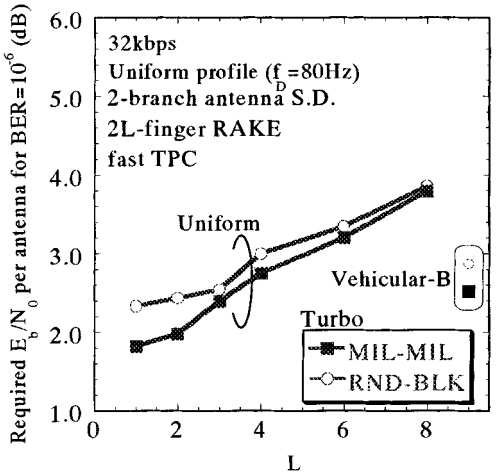

Fig. 15. Impact of number L of resolvable paths.

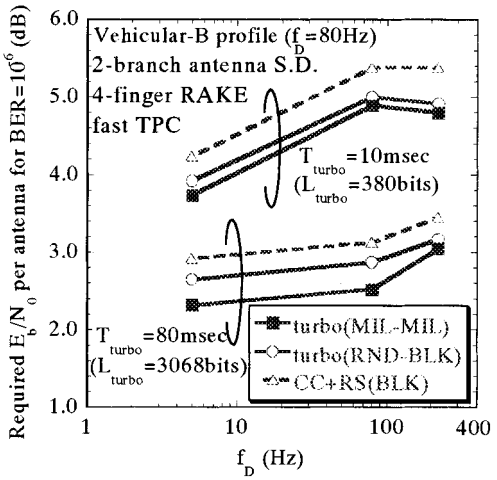

Fig. 14. Impact of fading maximum Doppler frequency f_D.

length increases, the performance superiority of MIL-MIL over RND-BLK strengthens. The gain of MIL-MIL over RND-BLK is about 0.4 dB at $T_{\text{turbo}} = 80$ ms ($L_{\text{turbo}} = 3068$ bits), while it is only 0.1 dB at $T_{\text{turbo}} = 10$ ms ($L_{\text{turbo}} = 380$ bits). Turbo coding (MIL-MIL) is even more powerful compared to CC+RS(BLK); the gain of turbo coding (MIL-MIL) against CC+RS(BLK) is about 0.6 dB at $T_{\text{turbo}} = T_{\text{channel}} = 80$ ms, while it is only 0.1 dB at $T_{\text{turbo}} = T_{\text{channel}} = 10$ ms.

Transmission performance is affected by the fading channel parameters, i.e., maximum Doppler frequency f_D, power-delay profile shape, and number of resolvable paths. How these factors affect the coding gain was examined. Fig. 14 shows the required received E_b/N_0 for a BER $= 10^{-6}$ as a function of f_D. The maximum Doppler frequency f_D (=vehicular speed/carrier wavelength) $=$ 111 Hz for 60 km/h and 2-GHz carrier frequency. The Vehicular B power-delay profile was assumed. While fast TPC works almost perfectly in the presence of very slow fading, e.g., $f_D < 10$ Hz, its tracking ability against fading wanes as fading increases. On the other hand, channel coding starts to work satisfactorily if the interleaving length is sufficiently long, e.g., $T_{\text{turbo}} = 80$ ms ($L_{\text{turbo}} = 3068$ bits). Therefore, the required E_b/N_0 only gradually increases with the value of f_D when $L_{\text{turbo}} = 3068$ bits. Fig. 14 also shows that turbo (MIL-MIL) gives larger coding gains compared to turbo (RND-BLK) and CC+RS (BLK) for all f_D values.

So far, we have considered only the Vehicular B power-delay profile. Here, we assume a uniform power-delay profile with L resolvable paths ($L = 1$–8). How the value of L impacts the required E_b/N_0 for BER $= 10^{-6}$ is plotted in Fig. 15. For comparison, the results for the Vehicular B power-delay profile are also plotted. It can be seen that the turbo-coding gain of MIL-MIL over RND-BLK is as much as 0.6 dB when $L = 1$ and falls as L increases; however, MIL-MIL is always superior to RND-BLK.

IV. Conclusion

Turbo coding is an attractive channel coding scheme for the third-generation mobile communications systems. The interleaving performed inside the turbo encoder plays an important role and requires a high degree of randomness while critical permutation patterns must be avoided. To meet these requirements, a multistage recursive block interleaver (MIL) was proposed in this paper. The BER and FER performance levels of turbo coding using MIL were evaluated by computer simulation assuming a power-controlled W-CDMA reverse link in frequency-selective Rayleigh-fading channels. We found that for 32-kbps data transmission, the gain of MIL over the pseudorandom interleaver is 0.4 dB at a BER $= 10^{-6}$assuming an interleaver length of 3068 bits and the Vehicular-B power-delay profile; the gain of MIL over the S-random interleaver exceeds 0.3 dB. We also found that the gain of turbo coding with MIL over the convolutional and RS concatenated code is 0.6 dB at a BER $= 10^{-6}$.

Acknowledgment

The authors thank Y. Okumura of the Radio Network Development Department and Dr. Y. Yamao and A. Fujiwara of Wireless Laboratories for their many helpful discussions and suggestions.

Authorized licensed use limited to: TOHOKU UNIVERSITY. Downloaded on March 07,2010 at 19:35:57 EST from IEEE Xplore. Restrictions apply.

REFERENCES

[1] F. Adachi, M. Sawahashi, and H. Suda, "Wideband DS-CDMA for next generation mobile communications," *IEEE Commun. Mag.*, vol. 36, pp. 56–69, Sept. 1998.

[2] E. Dahlman, B. Gudmundson, M. Nilsson, and J. Sköld, "UMTS/IMT-2000 based on wideband CDMA," *IEEE Commun. Mag.*, vol. 36, pp. 70–80, Sept. 1998.

[3] "Special Issue IMT-2000: Standards Efforts of the ITU," *IEEE Personal Commun.*, vol. 4, Aug. 1997.

[4] A. J. Viterbi, *CDMA: Principles of Spread Spectrum Communications*. Reading, MA: Addison-Wesley, 1995.

[5] C. Berrou, A. Glavieux, and P. Thitimajshima, "Near shannon limit error-correcting coding and decoding: Turbo-codes," in *Proc. IEEE ICC'93*, Geneva, Switzerland, May 23–26, 1993, pp. 1064–1070.

[6] L. C. Perez, J. Seghers, and D. J. Costello, "A distance spectrum interpretation of turbo codes," *IEEE Trans. Inform. Theory*, vol. 42, pp. 1698–1710, Nov. 1996.

[7] A. Fujiwara, H. Suda, and F. Adachi, "Turbo codes application to DS-CDMA mobile radio," *IEICE Trans. Fundamentals*, vol. E81-A, pp. 2269–2273, Nov. 1998.

[8] D. Divsalar and F. Pollara, "Multiple turbo codes for deep-space communications,", TDA Progress Rep. 42-121, May 15, 1995.

[9] T. Sohdoh, N. Nishinaga, and Y. Iwadare, "The new interleaver design of turbo codes for error floor improvement," in *Proc. 20th Symp. Information Theory and Its Application*, Matsuyama, Japan, Dec. 2–5, 1997, pp. 13–16.

[10] J. D. Andersen and V. V. Zyamlov, "Interleaver design for turbo coding," in *Proc. Int. Symp. Turbo Code*, Brest, France, Sept. 3–5, 1997, pp. 154–156.

[11] *Procedure for Evaluation of Transmission Technologies for FPLMTS*, Sept. 1995.

[12] S. Seo, T. Dohi, and F. Adachi, "SIR-based transmit power control of reverse link for coherent DS-CDMA mobile radio," *IEICE Trans. Commun.*, vol. E81-B, pp. 1508–1516, July 1998.

[13] Y. Honda and K. Jamal, "Channel estimation based on time-multiplexed pilot symbols,", IEICE Tech. Rep. RCS96-70, Aug. 1996.

Akira Shibutani received the B.S. and M.S. degrees from Keio University, Japan, in 1995 and 1997, respectively.

In 1997, he joined NTT Mobile Communications Network Inc., where he has been engaged in the research and development on turbo codes for third-generation mobile radio (W-CDMA). Since 2000, he has been with DoCoMo Communications Laboratories USA, Inc. His research interests lie in the area of adaptive channel coding and modulation.

Hiroshi Suda (M'85) received the B.S. and M.S. degrees from Yokohama National University, Yokohama, Japan, in 1982 and 1984, respectively.

In 1984, he joined the Electrical Communications Laboratories, Nippon Telegraph & Telephone Corporation (now NTT) and conducted research related to speech coding and FEC for second-generation mobile radio (PDC). From 1992 to 2000, he was with NTT DoCoMo, Inc., and studied turbo codes for third-generation mobile radio (W-CDMA). Since 2000, he has been with Wireless System Innovation Laboratory, NTT, where he is an Executive Research Engineer. His research interests lie in the area of radio resources management, wireless ad-hoc network architecture, adaptive channel coding and modulation, and transmit power control techniques.

Fumiyuki Adachi (M'79–SM'90) received the B.S. and Dr. Eng. degrees in electrical engineering from Tohoku University, Sendai, Japan, in 1973 and 1984, respectively.

In April 1973, he joined the Electrical Communications Laboratories, Nippon Telegraph & Telephone Corporation (now NTT) and conducted various types of research related to digital cellular mobile communications. From July 1992 to December 1999, he was with NTT Mobile Communications Network, Inc. (now NTT DoCoMo, Inc.), where he led a research group on wide-band/broadband CDMA wireless access for IMT-2000 and beyond. Since January 2000, he has been with Tohoku University, Sendai, Japan, where he is a Professor of electrical and communication engineering at the Graduate School of Engineering. His research interests are in OFDM, CDMA, and TDMA wireless access techniques, transmit/receive antenna diversity, adaptive antenna array, bandwidth-efficient digital modulation, and channel coding, with particular application to broadband mobile wireless communications systems. From October 1984 to September 1985, he was a United Kingdom SERC Visiting Research Fellow in the Department of Electrical Engineering and Electronics, Liverpool University. From April 1997 to March 2000, he was a Visiting Professor at Nara Institute of Science and Technology, Japan. He has published more than 180 papers in journals and more than 70 papers in international conferences.

Dr. Adachi was a Guest Editor of the IEEE JOURNAL ON SELECTED AREAS IN COMMUNICATIONS for special issues on Broadband Wireless Techniques (October 1999) and Wideband CDMA I (August 2000). He was a Corecipient of the IEEE Vehicular Technology Transactions Best Paper of the Year Award in 1980 and 1990. He received the Avant Garde Award in 2000. He is a member of the Institute of Electronics, Information and Communication Engineers of Japan (IEICE) and was a Corecipient of the IEICE Transactions Best Paper of the Year Award in 1996 and 1998.

Authorized licensed use limited to: TOHOKU UNIVERSITY. Downloaded on March 07,2010 at 19:35:57 EST from IEEE Xplore. Restrictions apply.